

# Mechanisms of photodissociative ionization of HCOOH: The heat of formation of COOH<sup>+</sup>

B. Ruscic, M. Schwarz, and J. Berkowitz

Chemistry Division, Argonne National Laboratory, Argonne, Illinois 60439

(Received 16 May 1989; accepted 8 August 1989)

The dissociative ionization of HCOOH to form COOH<sup>+</sup> + H + e has been reinvestigated. Experiments with DCOOH and HCOOD demonstrate that rearrangement competes with direct bond cleavage in this dissociation, even near threshold. Extrapolation of the photoion yield curve of COOH<sup>+</sup> to the background level is ambiguous. A photoelectron-photoion coincidence experiment was thereupon performed, to obtain a breakdown diagram. From the 0 K cross over energy of  $12.30 \pm 0.02$  eV, we infer  $\Delta H_f^0(\text{COOH}^+) = 143.2 \pm 0.5$  kcal/mol, and proton affinity (PA) (CO<sub>2</sub>) =  $129.2 \pm 0.5$  kcal/mol. Some possible mechanisms for the rearrangement process are explored, but the calculated barriers are too high to explain the observation.

## I. INTRODUCTION

The free radical COOH and its cation, COOH<sup>+</sup>, have both been the subjects of extensive investigation, but these studies have been almost completely disconnected from one another. The goal of the present article is to reexamine the heat of formation of COOH<sup>+</sup>, by photodissociative ionization of HCOOH. In the accompanying article,<sup>1</sup> we generate the neutral COOH and produce the cation by photoionization. The adiabatic ionization potential is, of course, the link between the heats of formation of COOH and COOH<sup>+</sup>. Prior studies related to  $\Delta H_f^0(\text{COOH}^+)$  are summarized below.

Pritchard *et al.*,<sup>2</sup> studied formic-*d* acid (DCOOH) by electron impact, and found an appearance potential of 12.4 eV for  $m/e = 46$  (DCOO<sup>+</sup>) and 12.8 eV for  $m/e = 45$  (COOH<sup>+</sup>), implying that DCOO<sup>+</sup> is the structure which is more stable. We shall return to this process in the present study, using photoionization, and demonstrate that in all likelihood a rearrangement occurs, so that the lower energy process corresponds to COOD<sup>+</sup>. More recently, Burgers *et al.*,<sup>3</sup> have offered evidence that HCOO<sup>+</sup> may be stable enough to survive at least 10 μs before rearranging to COOH<sup>+</sup>. A precise value of the heat of formation of COOH<sup>+</sup> implies an accurate value for the proton affinity of CO<sub>2</sub>. The structural question then can be rephrased—is the proton affinity greater at the C or the O site?

It is known from laboratory studies that a COOH<sup>+</sup> entity is formed in the proton transfer reaction between H<sub>3</sub><sup>+</sup> and CO<sub>2</sub>. Ion-molecule reactions are thought to play an important role in the formation of interstellar molecules.<sup>4</sup> COOH<sup>+</sup> is one of the key ions which are assumed as intermediates in a variety of gas phase reactions in interstellar clouds. In 1981, Thaddeus *et al.*,<sup>5</sup> detected some interstellar lines in the 85 GHz region which they tentatively assigned to HOCO<sup>+</sup> or HOCN. (Here, HOCO<sup>+</sup> is synonymous with COOH<sup>+</sup>.) Shortly thereafter, Bogey *et al.*,<sup>6,7</sup> obtained the submillimeter wave spectrum of COOH<sup>+</sup> in the laboratory, leading to the conclusion that three interstellar lines were indeed due to COOH<sup>+</sup>. Just after the initial observations of

Bogey *et al.*,<sup>6</sup> Amano and Tanaka<sup>8,9</sup> observed the ν<sub>1</sub> fundamental band of COOH<sup>+</sup> in laboratory investigations in the infrared, providing independent confirmation, and also detailed spectroscopic information from which a structure could be deduced.

Some *ab initio* calculations were reported at about the same time as these spectroscopic observations. Frisch *et al.*,<sup>10</sup> and later Yu *et al.*<sup>11</sup> calculated the geometric structures and stabilities of COOH<sup>+</sup> and HCO<sub>2</sub><sup>+</sup>. The two calculations agree rather well with one another. Their calculated structures and frequencies appear to be close to the experimental values of Amano and Tanaka.<sup>12</sup> According to these calculations, HCO<sub>2</sub><sup>+</sup> appears to be much less stable than COOH<sup>+</sup>, lying 105.8–108.7 kcal/mol higher according to Frisch *et al.*,<sup>10</sup> and 115.4 kcal/mol higher from the Yu *et al.*<sup>11</sup> results. Furthermore, the barrier to rearrangement (HCO<sub>2</sub><sup>+</sup> → COOH<sup>+</sup>) is small: 0.4–9.5 kcal/mol,<sup>10</sup> or 8.47 kcal/mol.<sup>11</sup> These calculations (see below) appear to be in fairly good agreement with experimental values for the proton affinity of CO<sub>2</sub>. If the calculated barrier to rearrangement is as accurate, the implication is that HCO<sub>2</sub><sup>+</sup> may be able to survive briefly, if prepared in a narrow energy range near its local minimum.

The most direct approach to the determination of the heat of formation of COOH<sup>+</sup> [and hence proton affinity (PA) (CO<sub>2</sub>)] is by measuring the dissociative ionization threshold from HCOOH by photoionization. It is the lowest energy fragmentation path. We are aware of three such measurements. Warneck<sup>13</sup> reported  $1009 \pm 3$  Å ≡  $12.29 \pm 0.03$  eV for this threshold. Villem *et al.*<sup>14</sup> obtained  $12.26 \pm 0.02$  eV as a photodissociative ionization threshold, and later Golovin *et al.*,<sup>15</sup> reported  $12.36 \pm 0.1$  eV. Apart from the small variation in threshold determination, there are two factors that neither Warneck nor the Russian workers appear to have taken into account in determining  $\Delta H_f(\text{COOH}^+)$ . The value for  $\Delta H_f(\text{HCOOH})$  used by Warneck is  $-3.919$  eV ≡  $-90.37$  kcal/mol, that by the Russian workers is  $-90.58$  kcal/mol. Both appear to be values for  $\Delta H_f^0(\text{HCOOH})$ , which is given in the NBS compilation<sup>16</sup> as  $-90.45$  kcal/mol. The corresponding value at 0 K is

– 88.79 kcal/mol.<sup>17</sup> Furthermore, there is no indication that either group considered the influence of the internal energy of  $\text{HCOOH}$  on the dissociative ionization threshold; the inference is that they performed a simple linear extrapolation. Such an onset should be shifted to higher energy by the internal thermal energy of  $\text{HCOOH}$  at 298 K, which amounts to 1.125 kcal/mol. These corrections are additive in determining  $\Delta H_{f_0}(\text{COOH}^+)$ . When taken into account, they yield  $143.4 \pm 0.5$  kcal/mol<sup>14</sup>,  $144.1 \pm 0.7$  kcal/mol<sup>13</sup> and  $145.7 \pm 2.3$  kcal/mol.<sup>15</sup> The corresponding proton affinities of  $\text{CO}_2$  at 0 K are 127.9, 127.2, and 125.6 kcal/mol. Proton affinities are generally evaluated at 298 K, for which the above values become  $129.0 \pm 0.5$ ,  $128.3 \pm 0.7$ , and  $126.7 \pm 2.3$  kcal/mol, respectively. Frisch *et al.*,<sup>10</sup> obtained 130.7 kcal/mol for this quantity, using their *ab initio* energies and empirically correlated frequencies, in good agreement with these experimental values.

## II. EXPERIMENTAL ARRANGEMENT

The basic photoionization mass spectrometric apparatus has been described previously.<sup>18</sup> Two different target chambers were employed. The experiment performed directly on  $\text{HCOOH}$ ,  $\text{HCOOD}$ ,  $\text{DCOOH}$ , and  $\text{DCOOD}$  utilized a conventional, more enclosed ionization chamber. As we shall illustrate below, there were some ambiguities in the threshold determinations from these species, which motivated us to measure a coincidence spectrum involving mass analyzed photoions and threshold photoelectrons. For this latter experiment, the target chamber contained a collimated hole structure on one side (for selecting near zero energy electrons) and a wire mesh opposite this side. The collimated hole structure is sometimes referred to as a steradiancy analyzer, and has been described previously.<sup>19</sup> A field of 6–8 V/cm was applied across this region, directing the near zero energy electrons through the collimated hole structure to a channeltron multiplier. The same field accelerated the ions through the wire mesh and into the focusing lens system, quadrupole mass filter, and a dynode multiplier. For these coincidence experiments, a detected photoelectron provided a start pulse, while the detected photoion provided the stop pulse. The coincidence measurements were performed on  $\text{HCOOH}$  and  $\text{DCOOD}$ , in the energy region where the first fragmentation occurs. Corresponding threshold photoelectron spectra were also obtained in this energy region. The  $\text{HCOOH}$  sample was from K&K Laboratories (99%), while  $\text{HCOOD}$ ,  $\text{DCOOH}$ , and  $\text{DCOOD}$  (all declared as 98% D) were obtained from Cambridge Isotope Laboratories. The samples were used without further purification, although the experiments with  $\text{HCOOD}$  and  $\text{DCOOD}$  required prolonged deuteration of the inlet line.

The primary light source utilized in these experiments was the many-lined emission from a discharge through molecular hydrogen. The wavelength resolution was  $0.28 \text{ \AA}$  [full width at half-maximum (FWHM)].

## III. EXPERIMENTAL RESULTS

### A. Photodissociative ionization of $\text{HCOOH}$ and $\text{DCOOH}$

In order to establish more precisely the heat of formation of  $\text{COOH}^+$ , and to examine the possibility of detecting

$\text{HCOO}^+$ , we reexamined the photodissociative onset for  $\text{COOH}^+$  from formic acid.

### 1. $\text{HCOOH}$ —the threshold for formation of $\text{COOH}^+$ / $\text{HCOO}^+$

The photoion yield curve for formation of ions with  $m/e = 45$  from  $\text{HCOOH}$  in the threshold region is shown in Fig. 1. Unlike the normal photoion yield curve of a fragment ion, which typically displays a linear postthreshold behavior, this fragmentation threshold curve has a tail ( $\sim 1015$ – $1010 \text{ \AA}$ ), followed by a linear ascent ( $\sim 1010$ – $1003 \text{ \AA}$ ), then a brief, steeper increase ( $\sim 1003$ – $1001 \text{ \AA}$ ) followed by a plateau ( $\sim 1000$ – $992 \text{ \AA}$ ) and another steep increase ( $\sim 992$ – $990 \text{ \AA}$ ), almost like step function behavior.

It is known that formic acid ( $\text{HCOOH}$ ) exists in *cis* and *trans* forms, differing in energy by about 4 kcal/mol.<sup>20</sup> One possible explanation for the step-like behavior is production of  $\text{HCOO}^+$  /  $\text{COOH}^+$  from each of these isomeric species, the difference in onsets representing the difference in energy between *cis* and *trans* forms. However, Boltzmann population arguments based on the energy gap between *cis* and *trans* forms of formic acid, enable us to conclude that the isomeric composition of formic acid vapor does not play a relevant role in these threshold measurements (the population of the higher energy *cis* form is too small to be significant). Another possible source of confusion is the presence of hydrogen-bonded dimers of formic acid in the vapor. Thomas<sup>21</sup> has examined this effect in the photoelectron spectrum of formic acid at several temperatures. At 300 K and 10 mTorr pressure, he calculates a trivial (nominally zero) dimer: monomer ratio, and our target pressure is  $\sim 2$  orders of magnitude lower. Hence, dimer effects can be safely excluded in our experiment. A third possibility, which seems extremely unlikely in view of the information concerning the relative stabilities of  $\text{COOH}^+$  /  $\text{HCOO}^+$  discussed in Sec. I, is that the two onsets are related to the thresholds for forma-

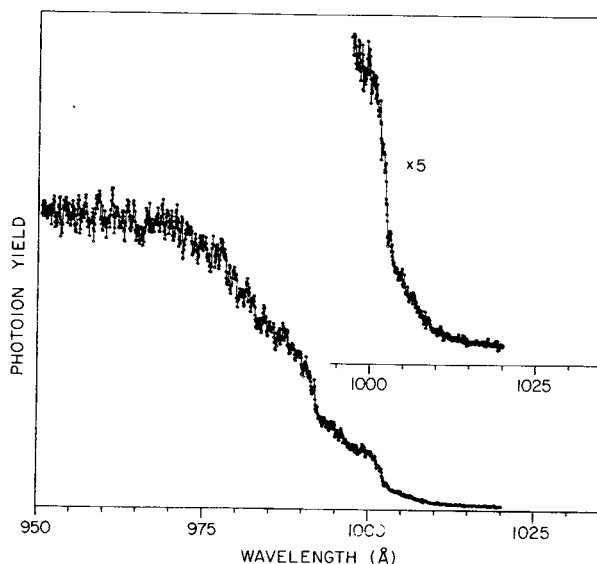


FIG. 1. The photoion yield curve of  $m/e = 45$  from  $\text{HCOOH}$ . This turns out to be the structure  $\text{COOH}^+$ , as established in the  $\text{DCOOH}$  experiment.

tion of these respective isomeric fragments. Finally, a possible explanation involves the excitation function, or probability of ionization, of the parent ion prior to dissociation. This total ionization cross section displays vibrational steps near the two aforementioned steep onsets.<sup>14</sup> As we shall see later, the two steep increases very nearly correspond to the formation of  $v' = 0$  ( $\sim 1001.4 \text{ \AA}$ ) and  $v' = 1$  ( $\sim 991.2 \text{ \AA}$ ) in the first excited state of  $\text{HCOOH}^+$ . Thus, we can tentatively extract a threshold for the formation of the fragment with  $m/e = 45$  by extrapolating the initial linear ascent ( $\sim 1010$ – $1003 \text{ \AA}$ ), rather than the steeper increase corresponding to the vibrational step. This procedure yields a value of  $1011.0 \pm 0.3 \text{ \AA} \equiv 12.264 \text{ eV}$ .

In order to further clarify the isomeric possibilities and to arrive at a more unambiguous explanation, we decided to examine the photodissociative ionization behavior of  $\text{DCOOH}$ .

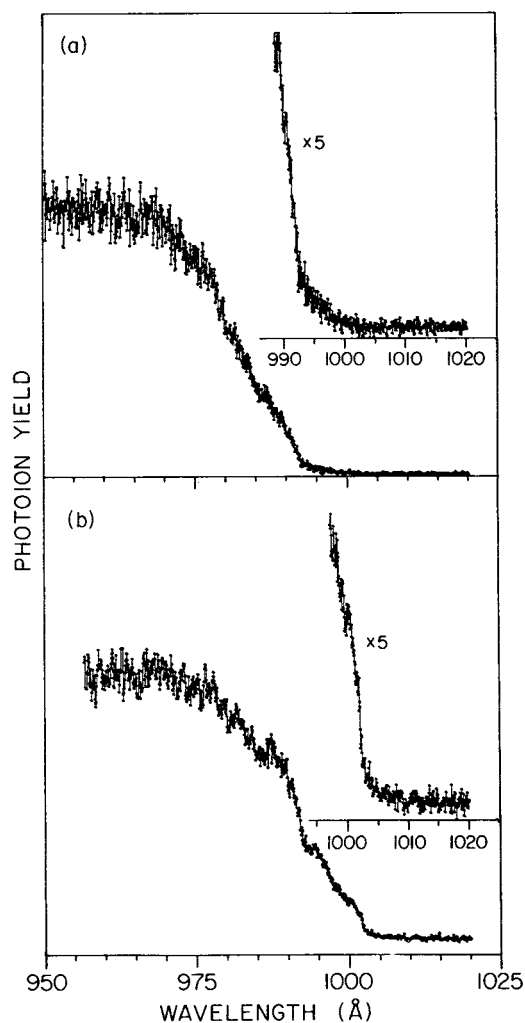


FIG. 2. (a) The photoion yield curve of  $m/e = 45$  from  $\text{DCOOH}$ . [The isotopic impurity  $\text{HCOOH}$  was 2%; the  $\text{COOH}^+$  ( $\text{HCOOH}$ ) contribution has been subtracted.] (b) The photoion yield curve of  $m/e = 46$  from  $\text{DCOOH}$ .

## 2. $\text{DCOOH}$ —the thresholds for formation of $m/e = 45$ and 46

The photoion yield curves for formation of ions with  $m/e = 45$  and  $m/e = 46$  are shown in Figs. 2(a) and 2(b), respectively. It is immediately apparent that the threshold region for  $m/e = 45$  does not display the two step onset, whereas  $m/e = 46$  does. The linearly extrapolated onset for  $m/e = 45$  to the background level occurs at  $\sim 993.5 \text{ \AA} \equiv 12.480 \text{ eV}$ , whereas the corresponding extrapolated onset for  $m/e = 46$  occurs at  $\sim 1003.0 \text{ \AA} \equiv 12.361 \text{ eV}$ . (It should be noted that, unlike  $m/e = 45$  in  $\text{HCOOH}$ , the  $m/e = 46$  fragment in  $\text{DCOOH}$  does not display a brief linear portion before the steep onset which corresponds to the first step.) The fact that the sharp, step-like increases are observed in the  $m/e = 46$  curve, but not in the  $m/e = 45$  curve, appears to be simply a consequence of the appearance energies of these fragments. The higher appearance energy of  $m/e = 45$  occurs at or beyond the second step.

If  $m/e = 46$  corresponded to a  $\text{DCOO}^+$  structure formed by simple bond rupture of the O–H bond, and  $\text{COOH}^+$  ( $m/e = 45$ ) resulted from simple bond rupture of the C–D bond in  $\text{DCOOH}^+$ , then we would be left with the conclusion that  $\text{DCOO}^+$ , having the lower threshold, is more stable than  $\text{COOH}^+$ . This conclusion seems extremely unlikely, in view of the extensive discussion on this point in Sec. I. It will be recalled, however, that these experimental observations are somewhat similar to those of Pritchard *et al.*<sup>2</sup> which led them to draw just such a conclusion. The *ab initio* calculations of Frisch *et al.*,<sup>10</sup> which compared so favorably with the newly found geometrical structure of  $\text{COOH}^+$  as well as the proton affinity of  $\text{CO}_2$ , and which predict that  $\text{HCOO}^+$  is less stable than  $\text{COOH}^+$  by 4.59–4.71 eV, and also the calculations of Yu *et al.*,<sup>11</sup> which find that  $\text{HCOO}^+$  is 4.99 eV less stable than  $\text{COOH}^+$ , appear to make this view untenable. Instead, our inference is that simple bond cleavage does not occur to form  $\text{DCOO}^+$ . Rather, rearrangement occurs in the dissociative ionization process, so that the  $m/e = 46$  ion appears at or near the threshold for  $\text{COOD}^+$ .

If thermochemistry alone governs the appearance potentials of  $\text{COOD}^+$  and  $\text{COOH}^+$ , then one can estimate the difference in appearance potentials from the respective zero-point energies. In the absence of secondary isotope effects, we can formally write

$$\text{AP}(\text{COOD}^+) = \Delta_e - \text{zpe}(\text{DCOOH}) + \text{zpe}(\text{COOD}^+), \quad (1)$$

$$\text{AP}(\text{COOH}^+) = \Delta_e - \text{zpe}(\text{DCOOH}) + \text{zpe}(\text{COOH}^+), \quad (2)$$

where AP stands for the appearance potential,  $\Delta_e$  is the energy from the bottom of the  $\text{DCOOH}$  potential energy surface to the bottom of the dissociative potential energy surface, and zpe refers to the respective zero point energies. Subtracting Eq. (1) from Eq. (2), we obtain

$$\text{AP}(\text{COOH}^+) = \text{AP}(\text{COOD}^+) + \text{zpe}(\text{COOH}^+) - \text{zpe}(\text{COOD}^+). \quad (3)$$

The *ab initio* calculations of Frisch *et al.*<sup>10</sup> provide us with

the vibrational frequencies of both COOH<sup>+</sup> and COOD<sup>+</sup>. Thus,  $zpe(\text{COOH}^+) = 4643 \text{ cm}^{-1}$ ,  $zpe(\text{COOD}^+) = 4034.5 \text{ cm}^{-1}$ , and their difference is  $608.5 \text{ cm}^{-1} \equiv 0.075 \text{ eV}$ , which is close to the experimentally determined difference, 0.118 eV, with the COOD<sup>+</sup> fragment appearing at the lower energy. This result implies that there is very little activation energy involved in the rearrangement.

Similarly, we can write

$$AP(\text{COOH}^+) = \Delta_e - zpe(\text{HCOOH}) + zpe(\text{COOH}^+). \quad (4)$$

Now subtracting Eq. (1) from Eq. (4), we obtain

$$\begin{aligned} AP(\text{COOH}^+/\text{HCOOH}) - AP(\text{COOD}^+/\text{DCOOH}) \\ = zpe(\text{DCOOH}) - zpe(\text{HCOOH}) \\ + zpe(\text{COOH}^+) - zpe(\text{COOD}^+). \end{aligned}$$

The vibrational frequencies of HCOOH and DCOOH are fairly well established experimentally.<sup>22</sup> The corresponding  $zpe$ s are 7161.5 and 6508.5  $\text{cm}^{-1}$ , and their difference, 653  $\text{cm}^{-1}$ , very nearly cancels the difference in  $zpe$ s between COOH<sup>+</sup> and COOD<sup>+</sup>, 608  $\text{cm}^{-1}$ . Thus,  $AP(\text{COOH}^+/\text{HCOOH})$  should be very nearly the same as  $AP(\text{COOD}^+/\text{DCOOH})$ , i.e., within 0.5 Å. This is not quite the case, as can be noted by comparing the threshold value in Fig. 1 with that in Fig. 2(b). These thresholds are also listed in Table I. The extrapolated threshold in Fig. 1 is 12.264 eV, that in Fig. 2(b) is 12.361 eV, a difference of almost 0.1 eV. Admittedly, this calculation combines experimental frequencies for the parent neutral species with *ab initio* calculated frequencies for the cation fragments, but the latter have been shown to be rather close to experimental values, where available, and the nature of the calculation allows for cancellation of errors. A plausible explanation is that the appearance of COOD<sup>+</sup> from DCOOH is very slightly ( $\sim 0.1 \text{ eV}$ ) retarded by the barrier to rearrangement.

These preliminary experiments provided us with an approximate value for the dissociative ionization threshold, but forced us to focus on two problems which needed to be solved before a more accurate appearance potential could be obtained.

(1) There appear to be two mechanisms, simple bond

cleavage and rearrangement, contributing to the fragment intensity near the ionization threshold. Can the superposition of the fragment intensities from these two processes confuse the extrapolation procedure used in determining the onset of fragmentation in HCOOH?

(2) In those instances where a "step behavior" is observed in the threshold region, the true fragmentation threshold occurs at lower energy than the steps, in a Frank-Condon gap. The intensity of the fragment ion is weak in this region, and the ion yield curve displays curvature, making a linear extrapolation uncertain.

In order to clarify the effects of total ionization probability, rearrangement and possible kinetic shift effects, additional experiments were performed.

## B. Photodissociative ionization of HCOOD and DCOOD

### 1. HCOOD

Our first approach was to examine the fragmentation thresholds for the remaining isotopic forms (HCOOD and DCOOD), and to use analogous zero point energy analyses, in the hope that a consistent appearance potential would emerge.

The photoion yield curves of CCOH<sup>+</sup> (HCOOD) and COOD<sup>+</sup> (HCOOD) are displayed in Figs. 3(a) and 3(b), respectively. In Figure 3(a) (extrapolated onset =  $993.2 \pm 0.6 \text{ Å} \equiv 12.483 \pm 0.008 \text{ eV}$ ), there is no step structure, just a linear postthreshold increase. In Fig. 3(b), one sees the two steps, and below them a short linear region with an extrapolated onset of  $1011.0 \pm 1.0 \text{ Å} \equiv 12.264 \pm 0.012 \text{ eV}$ . As in Figs. 2(a) and 2(b), the COOD<sup>+</sup> appears at lower energy than the COOH<sup>+</sup>, although in the DCOOH case it requires a rearrangement, whereas in the HCOOD case it could occur by simple bond cleavage. The appearance of step structure for the  $m/e = 46$  fragment, and its absence in the  $m/e = 45$  fragment, is again a consequence of the location of steps in the total ion yield. In the  $m/e = 45$  figures, the onset occurs beyond (at higher energy than) the steps in the total ion yield, and hence is absent.

TABLE I. Appearance energies and  $\Delta_e$  values for dissociative ionization of isotopic formic acid species.

Process	Appearance wavelength, (Å)	0 K appearance energy (eV) <sup>a</sup>	$\Delta_e$ (eV) <sup>a,b</sup>
HCOOH $\rightarrow$ COOH <sup>+</sup> + H + e	$1011.0 \pm 0.3$	$12.312 \pm 0.004$	$12.624 \pm 0.004$
DCOOH $\rightarrow$ COOD <sup>+</sup> + H + e	$1003.0 \pm 0.3$	$12.411 \pm 0.004$	$12.718 \pm 0.004$
DCOOH $\rightarrow$ COOH <sup>+</sup> + D + e	$993.5 \pm 0.3$	$12.529 \pm 0.004$	$12.760 \pm 0.004$
HCOOD $\rightarrow$ COOD <sup>+</sup> + H + e	$1011.0 \pm 1.0$	$12.315 \pm 0.012$	$12.623 \pm 0.012$
HCOOD $\rightarrow$ COOH <sup>+</sup> + D + e	$993.2 \pm 0.6$	$12.535 \pm 0.008$	$12.767 \pm 0.008$
DCOOD $\rightarrow$ COOD <sup>+</sup> + D + e	$1003.7 \pm 0.3$	$12.406 \pm 0.004$	$12.637 \pm 0.004$

<sup>a</sup> Vibrational frequencies for computation of zero point energies and internal thermal energy corrections of isotopic formic acid species taken from Ref. 22; vibrational frequencies of COOH<sup>+</sup> and COOD<sup>+</sup> for computation of zero point energies taken from Ref. 10. The appearance wavelengths are corrected to 0 K as described by P. M. Guyon and J. Berkowitz, *J. Chem. Phys.* **54**, 1814 (1971).

<sup>b</sup>  $\Delta_e$  (analogous to  $D_e$ ) is the difference in electronic energy from the minimum of the initial formic acid species to the minimum of the products.

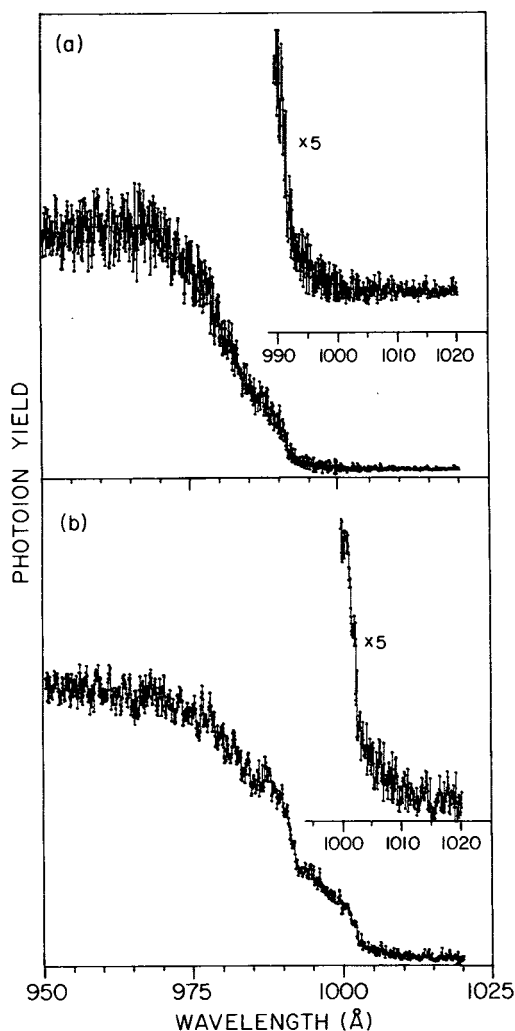


FIG. 3. (a) The photoion yield curve of  $m/e = 45$  from HCOOD. [The isotopic impurity HCOOH was 6.5%; the  $\text{COOH}^+$  (HCOOH) contribution has been subtracted.] (b) The photoion yield curve of  $m/e = 46$  from HCOOD. [A background at  $m/e = 46$  due to  $\text{HCOOH}^+$  (HCOOH) from the isotopic impurity is suppressed in this figure.]

## 2. DCOOD

The photoion yield curve of  $\text{COOD}^+$  (DCOOD) appears in Fig. 4. Between  $\sim 1010$ – $992 \text{ \AA}$ , one observes a somewhat curved ascent; between  $\sim 992$ – $990 \text{ \AA}$  there is a steeper increase, and below  $990 \text{ \AA}$ , a more gradual and linear portion. Prior to the present work, we were unaware of any photoelectron spectrum of DCOOD. We shall show below that the steep increase between  $\sim 992$ – $990 \text{ \AA}$  corresponds to the formation of  $v' = 1$  in the first excited state of  $\text{DCOOD}^+$ . It is interesting, and we believe significant, that no steep increase appears at the  $v' = 0$  position. We shall return to this point in the next section. The extrapolation of the photoion yield curve to the background level yields an appearance potential of  $1003.7 \pm 0.3 \text{ \AA} \equiv 12.353 \pm 0.004 \text{ eV}$ .

All of the appearance potentials mentioned above have subsequently been corrected for internal thermal energy of the neutral species, and are summarized in Table I. Also

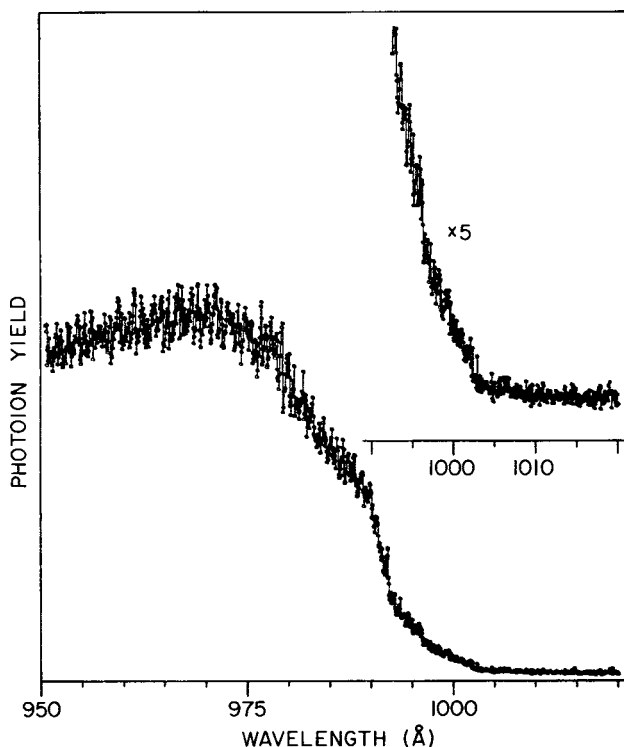


FIG. 4. The photoion yield curve of  $m/e = 46$  from DCOOD.

listed there are the values of  $\Delta_e$  obtained from each threshold. If each of these thresholds were thermochemically significant, the various  $\Delta_e$  values should be the same, apart from secondary isotope effects. The observed values can be placed into two categories. The lowest thresholds [ $\text{COOH}^+$  (HCOOH),  $\text{COOD}^+$  (HCOOD), and  $\text{COOD}^+$  (DCOOD)] have  $\Delta_e$  (avg) =  $12.628 \pm 0.013 \text{ eV}$ ; each is the lowest energy fragment, and can be produced by simple bond cleavage. The other three processes, with  $\Delta_e > 12.718 \text{ eV}$ , involve either rearrangement [ $\text{COOD}^+$  (DCOOH)] or correspond to a thermochemically higher energy process [ $\text{COOH}^+$  (DCOOH)], or both [ $\text{COOH}^+$  (HCOOD)].

## C. Photoion-photoelectron coincidence studies

The next approach was the photoelectron-photoion coincidence experiment. In this study, the number of true coincidences between near zero energy photoelectrons and parent photoions are recorded at a selected photon energy, and the process repeated for photoelectrons and fragment ions. The fraction of total coincidences for parent and fragment ions is plotted as a function of photon energy, producing a breakdown diagram. The cross-over point, where half the coincidences occur for parent ions and the other half for fragment ions, should be close to the 0 K appearance energy. Corrections (usually small) need to be made to take into account the initial thermal energy of the molecule, the transmission function of the steradiancy analyzer, and the energy deposition function, in this case the threshold photoelectron spectrum. In Figs. 5(c) and 6(c), the breakdown diagrams are displayed for HCOOH and DCOOD. Above each breakdown diagram is the corresponding photoion yield curve,

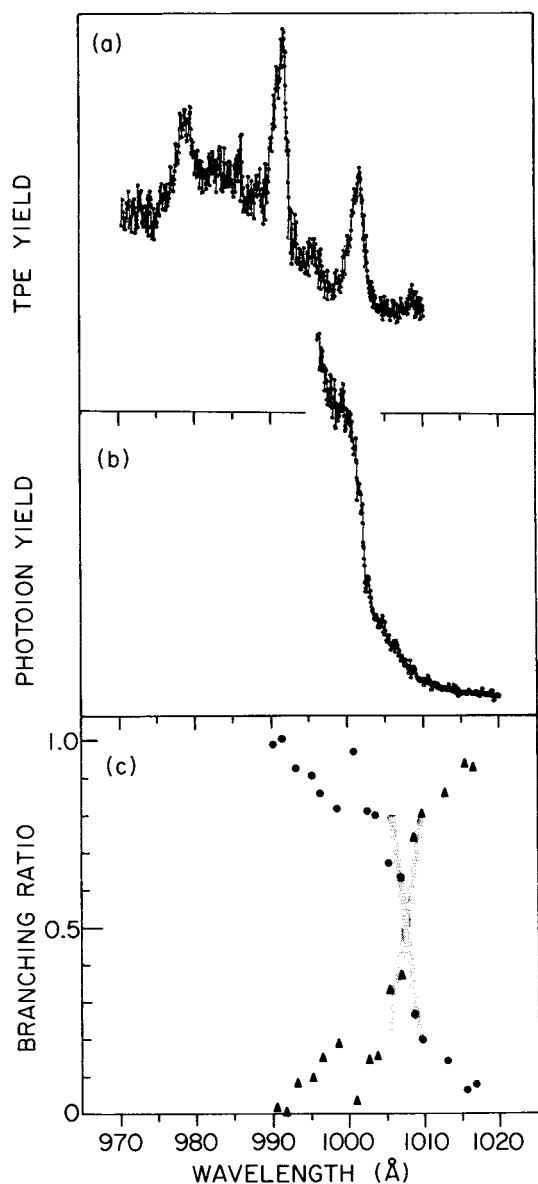


FIG. 5. (a) Threshold photoelectron spectrum of HCOOH. (b) Expanded photoion yield curve of  $\text{COOH}^+$  (HCOOH). (c) The breakdown diagram for the process  $\text{HCOOH}^+ \rightarrow \text{COOH}^+ + \text{H}$ . ● fraction of coincidences with  $\text{COOH}^+$  ( $m/e = 45$ ). ▲ fraction of coincidences with  $\text{HCOOH}^+$  ( $m/e = 46$ ).

i.e.,  $\text{COOH}^+$  (HCOOH) in Fig. 5(b) and  $\text{COOD}^+$  (DCOOD) in Fig. 6(b). In the upper panels [Fig. 5(a) and 6(a)] are the corresponding threshold photoelectron spectra (TPES). The TPES are quite similar to one another, and also similar to the He 1 PES of HCOOH (the second photoelectron band) given by Turner *et al.*<sup>23</sup> However, the resolution of the TPES spectra is about 18 meV, while that of Turner *et al.* is about 35 meV. Some splitting can be seen at the higher resolution, and a weak hot band is observed.

The difference in cross over wavelengths between HCOOH ( $\sim 1008 \text{ \AA}$ ) and DCOOH ( $\sim 996.5 \text{ \AA}$ ) is about  $11.5 \text{ \AA}$ . The cross over wavelength for HCOOH is very nearly equal to the 0 K threshold for this process listed in Table I. For DCOOD, however, the cross over wavelength is about

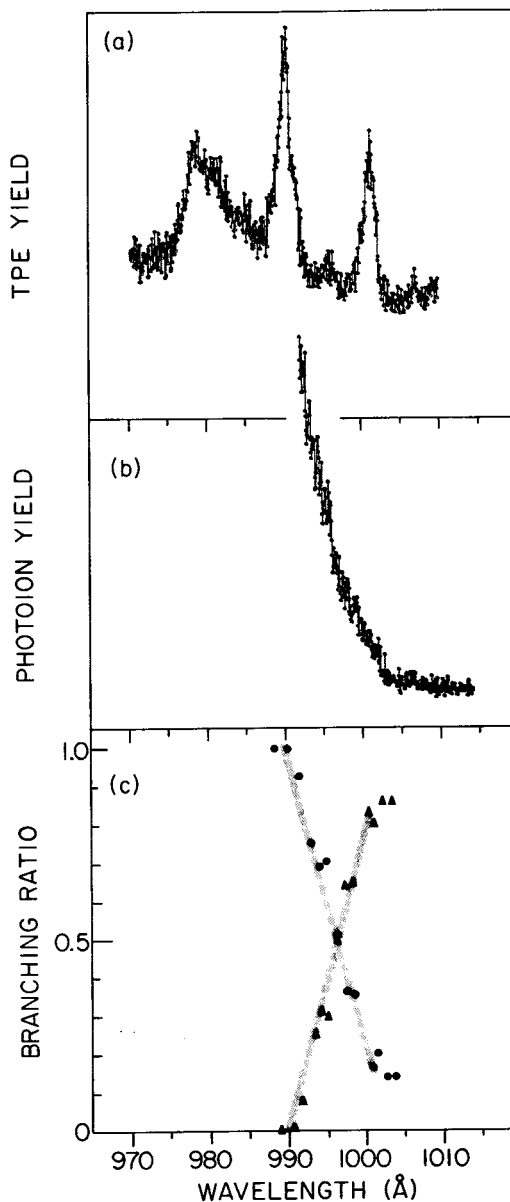


FIG. 6. (a) Threshold photoelectron spectrum of DCOOD. (b) Expanded photoion yield curve of  $\text{COOD}^+$  (DCOOD). (c) The breakdown diagram for the process  $\text{DCOOD}^+ \rightarrow \text{COOD}^+ + \text{D}$ . ● fraction of coincidences with  $\text{COOD}^+$  ( $m/e = 46$ ). ▲ fraction of coincidences with  $\text{DCOOD}^+$  ( $m/e = 48$ ).

$3.3 \text{ \AA}$  lower than the corresponding 0 K threshold. On the basis of zero point energy differences, the cross over wavelengths should differ by about  $7 \text{ \AA}$ . Thus,  $\text{COOD}^+$  (DCOOD) appears to have a delayed onset of about  $3.3\text{--}4.5 \text{ \AA}$ .

By comparing Fig. 5(a) and Fig. 1, it becomes apparent that  $v' = 0$  ( $\sim 1001.4 \text{ \AA}$ ) and  $v' = 1$  ( $\sim 991.2 \text{ \AA}$ ) in the TPES of HCOOH coincide with the two step-like features in the photoion yield curve of  $\text{COOH}^+$ .

In Fig. 6(a), one sees both the  $v' = 0$  ( $\sim 1001.1 \text{ \AA}$ ) and  $v' = 1$  ( $\sim 990.4 \text{ \AA}$ ) peaks in the TPES of DCOOD. As noted earlier, the steep increase in Fig. 6(b) correlates with the position of the  $v' = 1$  state, but no increase occurs at the



## ACKNOWLEDGMENT

This research was supported by the U.S. Department of Energy, Office of Basic Energy Sciences, under Contract No. W-31-109-Eng-38.

- <sup>1</sup>B. Ruscic, M. Schwarz, and J. Berkowitz, *J. Chem. Phys.* **91**, 6780 (1989).
- <sup>2</sup>H. Pritchard, J. C. J. Thynne, and A. G. Harrison, *Can. J. Chem.* **46**, 2141 (1968).
- <sup>3</sup>P. C. Burgers, J. L. Holmes, and J. E. Szulejko, *Int. J. Mass. Spectrom. Ion Proc.* **57**, 159 (1984).
- <sup>4</sup>E. Herbst and W. Klemperer, *Astrophys. J.* **185**, 505 (1973).
- <sup>5</sup>P. Thaddeus, M. Guelin, and R. A. Linke, *Astrophys. J.* **246**, L41 (1981).
- <sup>6</sup>M. Bogey, C. Demuynck, and J. L. Destombes, *Astron. Astrophys.* **138**, L11 (1984).
- <sup>7</sup>M. Bogey, C. Demuynck, and J. L. Destombes, *J. Chem. Phys.* **84**, 10 (1986).
- <sup>8</sup>T. Amano and K. Tanaka, *J. Chem. Phys.* **82**, 1045 (1985).
- <sup>9</sup>T. Amano and K. Tanaka, *J. Chem. Phys.* **83**, 3721 (1985).
- <sup>10</sup>M. J. Frisch, H. F. Schaefer III, and J. S. Binkley, *J. Phys. Chem.* **89**, 2192 (1985).
- <sup>11</sup>J. G. Yu, X. Y. Fu, R. Z. Liu, K. Yamashita, N. Koga, and K. Morokuma, *Chem. Phys. Lett.* **125**, 438 (1986).
- <sup>12</sup>Amano and Tanaka (Ref. 9) state that the calculated molecular structure is very close to the "experimental" structure of the ion, but that further measurements of the lines of the isotopic species, and also vibrationally excited states, are necessary to provide an improved molecular structure.
- <sup>13</sup>P. Warneck, *Z. Naturforsch. Teil A* **29**, 350 (1974).
- <sup>14</sup>Ya. Ya. Villem, M. E. Akopyan, and F. I. Vilesov, *High Energy Chem.* **9**, 356 (1975).
- <sup>15</sup>A. V. Golovin, M. E. Akopyan, F. I. Vilesov, and Yu. L. Sergeev, *High Energy Chem.* **13**, 171 (1979).
- <sup>16</sup>D. D. Wagman, W. H. Evans, V. B. Parker, R. H. Schumm, I. Halow, S. M. Bailey, K. L. Churney, and R. E. Nuttall, *J. Phys. Chem. Ref. Data* **11**, Suppl. 2, 2-77 (1982).
- <sup>17</sup>V. P. Glushko, L. V. Gurvich, G. A. Bergman, I. V. Veits, V. A. Medvedev, G. A. Khackhunuzov, and V. S. Yungman, *Termodinamicheski Svoistva Individual'nikh Veschestv* (Nauka, Moscow, 1979), Vol. 2.
- <sup>18</sup>S. T. Gibson, J. P. Greene, and J. Berkowitz, *J. Chem. Phys.* **83**, 4319 (1985).
- <sup>19</sup>R. Spohr, P. M. Guyon, W. A. Chupka, and J. Berkowitz, *Rev. Sci. Instrum.* **42**, 1872 (1972).
- <sup>20</sup>W. H. Hocking, *Z. Naturforsch. Teil A* **31**, 1113 (1976).
- <sup>21</sup>R. K. Thomas, *Proc. R. Soc. London Ser. A* **331**, 249 (1972).
- <sup>22</sup>R. C. Millikan and K. S. Pitzer, *J. Chem. Phys.* **27**, 1305 (1957); T. Miyazawa and K. S. Pitzer, *ibid.* **30**, 1076 (1958).
- <sup>23</sup>D. A. Turner, C. Baker, A. D. Baker, and C. R. Brundle, *Molecular Photoelectron Spectroscopy* (Wiley-Interscience, London, 1970), p. 158.
- <sup>24</sup>N. Heinrich and H. Schwarz, *Int. J. Mass. Spectrom. Ion Proc.* **79**, 295 (1987).
- <sup>25</sup>N. Heinrich, F. Louage, C. Lifshitz, and H. Schwarz, *J. Am. Chem. Soc.* **110**, 8183 (1988).
- <sup>26</sup>L. A. Curtiss (private communication).
- <sup>27</sup>M. C. Oliveira, T. Baer, S. Olesik, and M. A. Almoester-Ferreira, *Int. J. Mass Spectrom. Ion Proc.* **82**, 299 (1988).
- <sup>28</sup>M. W. Chase, Jr., C. A. Davies, J. R. Downery, Jr., D. J. Frurip, R. A. McDonald, and A. N. Syverud, *J. Phys. Chem. Ref. Data* **14**, Suppl. No. 1 (1985).
- <sup>29</sup>S. G. Lias, J. E. Bartmess, J. F. Liebman, J. L. Holmes, R. D. Levin, and W. G. Millard, *J. Phys. Chem. Ref. Data* **17**, Suppl. No. 1 (1988).
- <sup>30</sup>S. G. Lias, J. F. Liebman, and R. D. Levin, *J. Phys. Chem. Ref. Data* **13**, 695 (1984).
- <sup>31</sup>B. E. Ferguson (private communication); N. G. Adams, D. Smith, M. Tichy, G. Javahery, N. D. Twiddy, and E. E. Ferguson, *J. Chem. Phys.* **91**, 4037 (1989).